Serican Journal of Medicine
2025, VOL. 2, NO. 2, 23642
https://doi.org/10.17161/sjm.v2i2.23642

The Safety and Protective Effects of Intravitreal Injection of Human Adipose-Derived Mesenchymal Stem Cells in a Rat Model of Retinal Ischemia/Reperfusion Injury

Baiyu Hu, Jing Shu, Hanying Fan, Mei Xin and Liuzhi Zeng*

Department of Ophthalmology, Chengdu First People's Hospital, Chengdu 610095, China.
***Correspondence to:** Liuzhi Zeng, Department of Ophthalmology, Chengdu First People's Hospital, No.18 Wanxiang North Road, High-tech Zone, Chengdu, Sichuan Province 610095, China. Email: 676681961@qq.com

ABSTRACT

Purpose: The purpose of this study was to evaluate the safety and protective effects of intravitreal injection of human adipose-derived mesenchymal stem cells (ADMSCs) in a rat model of retinal ischemia/reperfusion (I/R) injury induced by anterior chamber perfusion.

Methods: Two weeks after induction of I/R injury, rats received a single intravitreal injection of human ADMSCs at doses of 2×10^4 cells or 5×10^4 cells suspended in 3 µL saline. Control rats received 3 µL saline or no injection. Retinal and optic nerve changes were assessed two weeks after injection using immunofluorescence, hematoxylin and eosin staining, toluidine blue staining, and polymerase chain reaction to evaluate inflammation-related and neurotrophic factors.

Results: Intravitreal injection of human ADMSCs significantly reduced the number of apoptotic retinal ganglion cells after I/R injury, preserved the ganglion cell layer, and increased expression of neurotrophic factors such as brain-derived neurotrophic factor and insulin-like growth factor 1. The high-dose group (receiving 5×10^4 cells) demonstrated superior neuroprotective effects compared to the low-dose group (receiving 2×10^4 cells) as evidenced by less retinal ganglion cell apoptosis. In addition, histopathological analysis revealed localized tissue remodeling and increased microglial infiltration, particularly in the low-dose group.

Conclusion: The safety of intravitreal human adipose-derived mesenchymal stem cell transplantation requires further investigation, particularly concerning potential proliferative responses and their long-term effects. In addition, the optimal dosage of adipose-derived mesenchymal stem cells needs to be explored to balance therapeutic efficacy and minimize adverse outcomes, which were associated with structural retinal damage. In addition, the high-dose group exhibited a potential risk of inflammation or maladaptive changes.

ARTICLE HISTORY
Received: Feb. 20, 2025
Revised: Feb. 22, 2025
Accepted: Feb. 24, 2025

KEYWORDS
ischemia/reperfusion, adipose-derived mesenchymal stem cells, safety, efficacy

Introduction

Glaucomatous optic nerve damage is a neurodegenerative condition characterized by progressive loss of retinal ganglion cells and axons, ultimately resulting in irreversible vision loss [1, 2]. While current therapeutic approaches focus on lowering intraocular pressure (IOP) through medications or surgery, these interventions do not address the underlying neurodegeneration. Consequently, recent research has shifted toward developing neuroprotective strategies, such as delivering neurotrophic factors [1], inhibiting pro-apoptotic pathways, suppressing inflammation, and reducing oxidative stress. Among these, cell therapy has emerged as a promising avenue for neuroprotection and optic nerve regeneration [3]. Mesenchymal stem cells (MSCs) are a heterogeneous group of stromal cells capable of multi-direction-al differentiation into adipocytes, osteoblasts, and chondrocytes [3-5]. Compared to bone marrow-de-rived stem cells, adipose-derived mesenchymal stem cells (ADMSCs) can be obtained in larger quantities and exhibit an enhanced capacity for cytokine secre-tion, thus having better therapeutic and regenerative potentials [6, 7]. ADMSCs are widely recognized for their anti-inflammatory, anti-fibrotic, anti-apop-totic, and pro-angiogenic properties, making them promising candidates for cell-based therapies in both retinal and optic nerve diseases [8]. Despite their therapeutic potential, the

safety of intravitreal injection of ADMSCs remains controversial [8]. While some clinical trials have reported the safety and efficacy of ADMSCs in retinal and optic nerve diseases [9], other studies have highlighted potential complications, including reactive gliosis, severe inflammatory responses, and retinal damage [10]. For instance, intravitreal injection of MSCs has been associated with retinal structural damage and visual function loss in preclinical models [11, 12]. Some researchers have proposed that implanting MSCs in the choroid or subfascial space could represent a safer alternative for treating retinal degeneration by avoiding direct contact with the retinal tissue [13, 14]. These conflicting findings underscore the need for further evaluation of the safety and potential risks of intravitreal ADMSC therapy before its clinical application. The objective of this study was to evaluate the safety and protective effects of intravitreal injection of human ADMSCs in a preclinical rat model of retinal ischemia/reperfusion (I/R) injury. Specifically, we assessed the fundus morphology and histological changes in the retina and optic nerve following the injection of ADMSCs. Given the ultimate goal of translating stem cell therapies to human clinical use, human ADMSCs were chosen to evaluate their safety and protective effects in a xenogeneic environment.

Materials and Methods

Animal study: The Institutional Animal Care and Use Committee of the Institute of Laboratory Animal Science, Sichuan Academy of Medical Sciences, and the Sichuan Provincial People's Hospital approved the animal study protocol (#2022 No. 005). Sprague-Dawley (SD) rats (all females) with a body weight of about 200-240 g were purchased from Hunan Slaughter Kingda Laboratory Animal Co Ltd (Hunan Province, China) and maintained according to the protocol approved by the local ethics committee of Hunan Science and Technology Department (Hunan Province, China). Experiments were conducted at the Sichuan Provincial People's Hospital laboratory, where rats were fed with standard chow. Rats had unrestricted access to food and drinking water during a 12-hour dark/light cycle under the constant supervision of trained staff. Fourteen days after ischemia/reperfusion (I/R) injury, rats received a single intravitreal injection of human ADMSCs or saline. ADMSCs were suspended in 3 µL saline, with two doses tested: 5×10^4 cells (I/R+ ADMSC high-dose group, n = 6 rats) and 2×10^4 cells (I/R + ADMSC low-dose group, n = 6 rats). A sham injection group received an intravitreal injection of 3 µL saline (I/R+ Saline group, n = 6 rats, excluding the one with adverse effects). Another group received I/R injury but not intravitreal injection (I/R group, n = 6 rats). A normal control group did not receive I/R injury or intravitreal injection (Normal Control group, n = 6 rats).

MSCs isolation and culture: Human ADMSCs were chosen to better simulate potential clinical applications and evaluate their behavior in a xenogeneic environment. Human ADMSCs were provided by Beijing Regenerative Biotechnology Research Institute Co, Ltd. (Beijing, China). The human anatomic substance study was approved by the ethics committee of the Sichuan Provincial People's Hospital. Human ADMSCs were obtained from human abdominal adipose tissues harvested during plastic surgeries, with the donors' written consent. The procedures to obtain ADMSCs are briefly described as the following. Adipose tissues were washed twice with saline to remove residual blood and debris. The adipose tissues were resuspended in two-times volumes of saline containing 50 µg/mL gentamicin sulfate and centrifuged at 500 × g for 10 minutes. The fatty layer was removed, and the precipitated layer was collected and washed twice with saline. The precipitated layer was digested with a solution containing 0.15 mg/mL collagenase NB 1 (SERVA, Heidelberg, Germany) and 50 IU/mL recombinant human DNase-I (ProSpec, Ness Ziona, Israel) in a water bath at 37°C for 30 minutes, with vigorous shaking every 5 minutes. Suspended flocculants were removed, and the mixture was filtered through a 200-µm mesh sieve to collect the filtrate. The filtrate was centrifuged at 1000 rounds per minute for 10 minutes. The supernatant was discarded, and the pellet was resuspended in phosphate-buffered saline (PBS) and allowed to stand for 10 minutes. The supernatant was discarded, and the pellet was centrifuged at 300 × g for 10 minutes. The supernatant was discarded, and the cell pellet was resuspended in UltraCULTURE medium (Lonza, Walkersville, MD, USA) supplemented with 2% Ultroser™ G serum substitute (PALL, Port Washington, NY, USA). The cell density was adjusted to 5×10^5 cells/mL and seeded into 175 cm^2 tissue culture flasks (EasyFlask, NUNC, Roskilde, Denmark). The cells were cultured with half-volume medium changes at 24 and 36 hours, a full-volume medium change

at 48 hours, and every other day thereafter until they reached 70-80% confluence. At harvesting time, the culture supernatant was discarded, and the cells were washed once with saline. Cells were digested with 0.25% trypsin solution (Biological Industries, Beit HaEmek, Israel) for 5 minutes at room temperature. The digestion was terminated with 1 mL of peptidase inhibitor solution (Sigma-Aldrich, St. Louis, MO, USA). The harvested cells were centrifuged at 400 × g for 5 minutes, washed twice with saline, and filtered through a 100-μm nylon cell sieve. The collected cells were designated as passage zero (P0) ADMSCs and resuspended in UltraCULTURE medium. P0 ADMSCs were harvested at 70-80% confluence in about 3 days and seeded at 10,000 cells/cm^2 for another 3 days. The ADMSCs were harvested as passage 1 (P1). After another 3-day culture, the ADMSCs were harvested as passage 2 (P2). P2 ADMSCs were frozen at 1×10^7 cells/mL in serum-free cryoprotectant (Cellbanker II, Tokyo, Japan).

Retinal I/R Model: Rats were under general anesthesia induced with 0.3% pentobarbital sodium administered via intraperitoneal injection at a dose of 40-50 mg/kg body weight. Before induced I/R injury, anterior segment examination and fundus photography were performed to exclude rats with keratopathy, cataracts, or fundus abnormalities. None of the rats showed any abnormalities, thus they were all included in the study. After local disinfection with povidone-iodine and rinsing with physiological saline, a 30-G indwelling needle was carefully inserted into the anterior chamber of one eye (only one eye was used to generate I/R injury), avoiding damage to the iris. The indwelling needle was secured and connected to the perfusion system. The perfusion system was set up using 250 mL saline. To maintain high intraocular pressure (IOP), the saline reservoir was elevated to a height of 110 cm above the eye, generating a hydrostatic pressure gradient. High IOP was maintained for 90 minutes, and retinal ischemia was confirmed by iris whitening and the loss of the red reflex from the fundus. IOP was terminated to allow blood reperfusion. Rats recovered from anesthesia were returned to the cages for two weeks.

Intravitreal injection: Previous studies have demonstrated that intravitreal interventions within two weeks after ischemia/reperfusion (I/R) injury effectively target the acute inflammatory phase and prevent progressive neurodegeneration [15-17]. Two weeks after the I/R injury, rats were under general anesthesia induced using isoflurane at a concentration of 2%, mixed with oxygen at a flow rate of 1 L/min. The eye with I/R injury was disinfected with a povidone-iodine solution and dried using sterile gauze. Under an operating microscope, a micro-glass tube was inserted into the vitreous cavity approximately 0.5 mm behind the corneoscleral limbus. The other end of the glass tube was connected to a 10-μL microsyringe, which delivered 3 μL of ADMSCs (2×10^4 or 5×10^4 cells suspended in saline) or saline only. The injection was performed slowly to minimize mechanical damage, and the micro-glass tube was kept in place for 10 seconds after injection to prevent liquid reflux upon withdrawal. Following injection, levofloxacin eye ointment was applied to the conjunctival sac to prevent infection. Rats were returned to the cages. Two weeks later, all rats were euthanized, and the eyes were collected for histological and molecular analyses.

Hematoxylin and eosin (H&E) staining: Eye tissue samples were fixed in 4% paraformaldehyde for 24 hours and subsequently processed using standard protocols, including paraffin embedding, sectioning at a thickness of 4 μm, deparaffinization with xylene, and rehydration through graded ethanol solutions to distilled water. Tissue sections were stained with hematoxylin (hematoxylin solution, Sigma-Aldrich, St. Louis, MO, USA) for 3-5 minutes to highlight cell nuclei, followed by rinsing with running tap water for 1-2 minutes to remove excess stain. Tissue sections were briefly differentiated in 1% acid alcohol (1% HCl in 70% ethanol) for 5-10 seconds to enhance nuclear clarity, then rinsed again under running tap water to restore the blue color. Subsequently, tissue sections were stained with eosin (eosin Y solution, Sigma-Aldrich, St. Louis, MO, USA) for 2-5 minutes to counterstain the cytoplasm and extracellular matrix. Excess eosin was removed by rinsing briefly in distilled water. After staining, the sections were dehydrated through an ascending ethanol series (70%, 95%, and 100%) for 2-3 minutes at each concentration and cleared in xylene for 5 minutes. Finally, the sections were mounted with neutral resin (Thermo Fisher Scientific, Waltham, MA, USA) and allowed to dry before microscopic examination.

Immunofluorescent staining: Eye tissue sections were treated with antigen retrieval performed by placing the slides in Tris-ethylenediaminetetraacetic

acid (Tris-EDTA) buffer, pH 9.0, at 100 °C for 5 min. The slides were incubated in serum-free conditions, after which they were encircled with a histochemical pen and treated with bovine serum albumin (BSA, 3% or 10% depending on the antibody sources). Sections were incubated with primary antibodies overnight at 4°C in a wet box, including anti-Brain-3A (Brn-3a) (RRID: GB111661, Servicebio, Wuhan, China), rabbit anti-Ki67 (RRID: GB111141 Servicebio, Wuhan, China), rabbit anti-Ionized Calcium-Binding Adapter Molecule 1 (Iba1) (RRID: AB_3070606, HUABIO, Hangzhou China), and anti-Glial Fibrillary Acidic Protein (GFAP) (RRID: GB11096, Servicebio, Wuhan, China). After washing three times, Alexa Fluor 488-conjugated anti-rabbit IgG secondary antibodies (RRID: GB21303, Servicebio, Wuhan, China) were incubated for 50 minutes at room temperature in the dark. The nuclei were counterstained with 4',6-diamidino-2-phenylindole (DAPI).

Immunohistochemical staining: Eye tissue sections were treated with antigen retrieval performed by placing the slides in Tris-ethylenediaminetetraacetic acid (Tris-EDTA) buffer, pH 9.0, at 100 °C for 5 min. To block nonspecific binding, 3% BSA was applied dropwise to cover the tissues evenly, followed by a 30-minute incubation at room temperature. Primary antibodies were applied to the tissue sections, including anti-Epithelial Membrane Antigen 1(AE1) (RRID: GB113603)(1:2000), Synaptophysin (RRID: GB111853) (1:500) and vimentin(RRID: GB111308) (1:1000). Negative controls were set up using a non-immune serum to replace the primary antibodies. The slides were incubated overnight at 4°C in a humidified chamber. After washing three times, secondary antibodies conjugated to horseradish peroxidase (HRP) (RRID: GB21303, Servicebio, Wuhan, China) were added dropwise to the tissue sections and incubated for 50 minutes at room temperature. Afterward, the slides were rinsed with PBS to remove unbound antibodies. For 3,3'-Diaminobenzidine (DAB) staining, a freshly prepared 3,3'-Diaminobenzidine (DAB) solution was applied to the tissue sections, and the color development was monitored under a microscope until the positive signals appeared as brownish-yellow. The reaction was terminated by rinsing the slides with tap water. Cell nuclei were counterstained with hematoxylin for three minutes, followed by rinsing with tap water. The sections were then differentiated, rinsed, and returned to a bluing solution before mounting for imaging. A semi-quantitative grading system (0–3) was established for toluidine blue-stained optic nerve sections: 0 = no apparent damage, 1 = mild damage, 2 = moderate damage, and 3 = severe damage. For each specimen, three fields were examined at the same magnification (400×), and the average score was calculated.

Terminal deoxynucleotidyl transferase dUTP nick end labeling (TUNEL) staining: TUNEL assay kits were obtained from Servicebio, Wuhan, China. Eye tissue sections were treated with proteinase K diluted in PBS (1:1000) for 22 minutes at 37°C. The membrane-breaking solution (0.1% Triton X-100) was applied and incubated for 20 minutes at room temperature. TUNEL reaction buffer was equilibrated for 10 minutes at room temperature, followed by the addition of terminal deoxynucleotidyl transferase (TDTase) and dUTP, and incubation at 37°C for 1 hour. The nuclei were counterstained with DAPI.

RNA extraction and quantitative real-time polymerase chain reaction (qPCR): Retina tissues from six eyes in each group were harvested for RNA isolation using the Servicebio® RT First Strand cDNA Synthesis Kit (Servicebio, Wuhan, China). Reverse transcription was then performed using this kit according to the manufacturer's protocol. The reaction conditions were set as follows: 25 °C for 5 minutes, 42 °C for 30 minutes, and 85 °C for 5 seconds. PCR primers were synthesized to detect the mRNA expression levels of vascular endothelial growth factor (VEGF), insulin-like growth factor 1 (IGF-1), brain-derived neurotrophic factor (BDNF), and tumor necrosis factor-alpha (TNFα) (Table 1. Sequences of PCR primers). qPCR was then conducted under the following conditions: pre-denaturation at 95 °C for 30 seconds, denaturation at 95 °C for 15 seconds, annealing and derivatization at 60 °C for 30 seconds for 40 cycles, and fluorescence collection at increments of 0.5 °C from 65 °C to 95 °C.

Toluidine blue staining: A tissue sample of about 1 mm adjacent to the posterior surface of the eyeball was collected to observe the number of optic nerve fibers. The sample was fixed in 0.1 M phosphate buffer (pH 7.4) containing 1% osmium acid at room temperature for 2 hours. After fixation, the sample was dehydrated at room temperature and embedded in paraffin. The sample was then sectioned and stained with Toluidine blue solution (Servicebio, Wuhan, China).

Table 1. PCR Primer Sequences for Target Genes in ADMSC Treatment.

Gene	Primer Name	Primer Sequence (5'→3')	Product Size (bp)	Tm (°C)
TNF-α	TNF-α-F	CCAGGTTCTCTTCAAGGGACAA	80	60
	TNF-α-R	GGTATGAAATGGCAAATCGGCT		60
IGF-1	IGF-1-F	AAAATGAGCGCACCTCCAAT	149	60
	IGF-1-R	ACGAACTGAAGAGCGTCCACC		60
VEGF	VEGF-F	TGTGAGCCTTGTTCAGAGCG	197	60
	VEGF-R	GGTCTAGTTCCCGAAACCCTGA		60
BDNF	BDNF-F	GTGTGACAGTATTAGCGAGTGGG	221	60
	BDNF-R	ACGATTGGGTAGTTCGGCATT		60
GAPDH	GAPDH-F	CTGGAGAAACCTGCCAAGTATG	138	60
	GAPDH-R	GGTGGAAGAATGGGAGTTGCT		60

Statistical analyses: Statistical analyses were performed using SPSS 27 statistical software. Data are presented as mean ± standard deviation (SD). Normality was assessed using the Shapiro-Wilk test, and homogeneity of variance was evaluated by Levene's test. For comparisons between multiple groups, one-way analysis of variance (ANOVA) followed by Tukey's post hoc test was used for normally distributed data. If the data did not follow a normal distribution, the Kruskal-Wallis H test was conducted, followed by Dunn's post hoc test for multiple comparisons. For pairwise comparisons, normally distributed data were analyzed using the independent samples Student's t-test, while the Mann-Whitney U test was used for non-normally distributed data. Correlation analyses were performed using the Pearson correlation coefficient for normally distributed data and the Spearman correlation coefficient for non-normally distributed data. A P-value < 0.05 was considered statistically significant.

Results

Two weeks after ADMSC injection, the retinal structure and the number of retinal ganglion cells (RGCs) in the ganglion cell layer (GCL) were examined. In the GCL of normal rats, the retinal structure appeared intact, with RGCs arranged tightly in a single layer. Individual cells possessed clear boundaries and comparatively large, round, or oval nuclei (Figure 1A). In contrast, the I/R group exhibited multiple layers in both the inner and outer nuclear layers (Figure 1A), partial RGC loss (Figure 1C), and overall thinning of the retina (Figure 1D). To further assess the integrity of the optic nerve among different experimental groups, toluidine blue staining was performed (Figure 1B). In the normal control group, the optic nerve displayed uniform axonal structures characterized by tightly packed axon bundles and well-preserved myelin sheaths. However, following I/R, significant alterations were observed in the model group, including axonal disruption, areas of axon

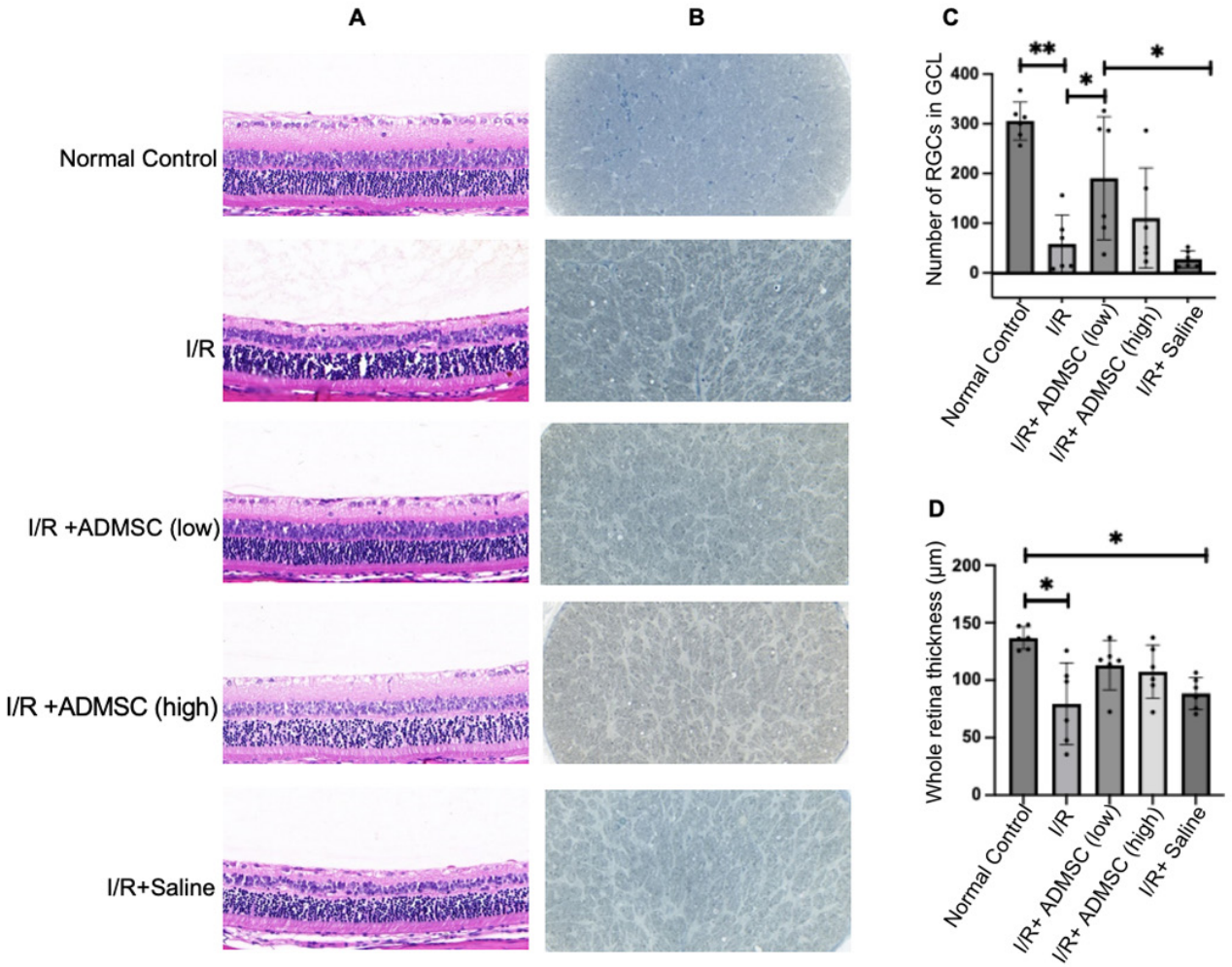

Figure 1. Results at two weeks after intravitreal delivery of ADMSCs in rats. (A) Hematoxylin and eosin (H&E) staining of retinal sections; scale bar, 20 μm; digital magnification, x400. (B) Toluidine blue staining of the optic nerves. (C) Quantitative analysis of retinal ganglion cells (RGCs) in the ganglion cell layer (GCL); * $p < 0.05$ and ** $p < 0.01$ by Mann-Whitney U test ($n = 6$); a significant difference ($p < 0.05$) was found between the I/R+ADMSC (low) and I/R+ Saline groups. (D) Representative retinal thickness of each group; * $p < 0.05$.

loss, gliotic scarring, and fiber thickening, all distinctly highlighted by toluidine blue staining. These prominent structural abnormalities indicate that I/R-induced injury exerts a notable impact on optic nerve integrity. Semi-quantitative scoring of toluidine blue-stained optic nerve sections found that the median scores (range) for each group were as follows: Normal Control group, 0 [0, 0]; I/R group, 1.5 [1, 2.25]; I/R + ADMSC low-dose group, 2 [1, 2.25]; I/R + ADMSC high-dose group, 2 [1.75, 3]; and I/R + Saline group, 1.5 [1, 3]. There were not any statistically significant differences among the groups (Kruskal-Wallis test, $p > 0.05$), suggesting that there were no discernible histomorphological improvements in the optic nerves following stem cell therapy.

The I/R+ADMSC low-dose group exhibited a significantly higher number of RGCs compared to the I/R or I/R+Saline group (Figure 1C, $p < 0.05$). However, no statistically significant difference was observed between the I/R+ADMSC high-dose group and the I/R or I/R+Saline group (Figure 1C, $p > 0.05$). The whole retina thickness was significantly lower in the I/R and I/R+Saline groups compared to the normal control group ($p < 0.05$). The whole retina thickness was thicker in the I/R+ADMSC groups than in the I/R or I/R+Saline group, though the differences were not statistically significant (Figure 1D, $p > 0.05$).

In the retina, glial cells play a pivotal role in the immune response and retinal homeostasis [18]. In the I/R+ADMSC groups, astrocytes were predomi-

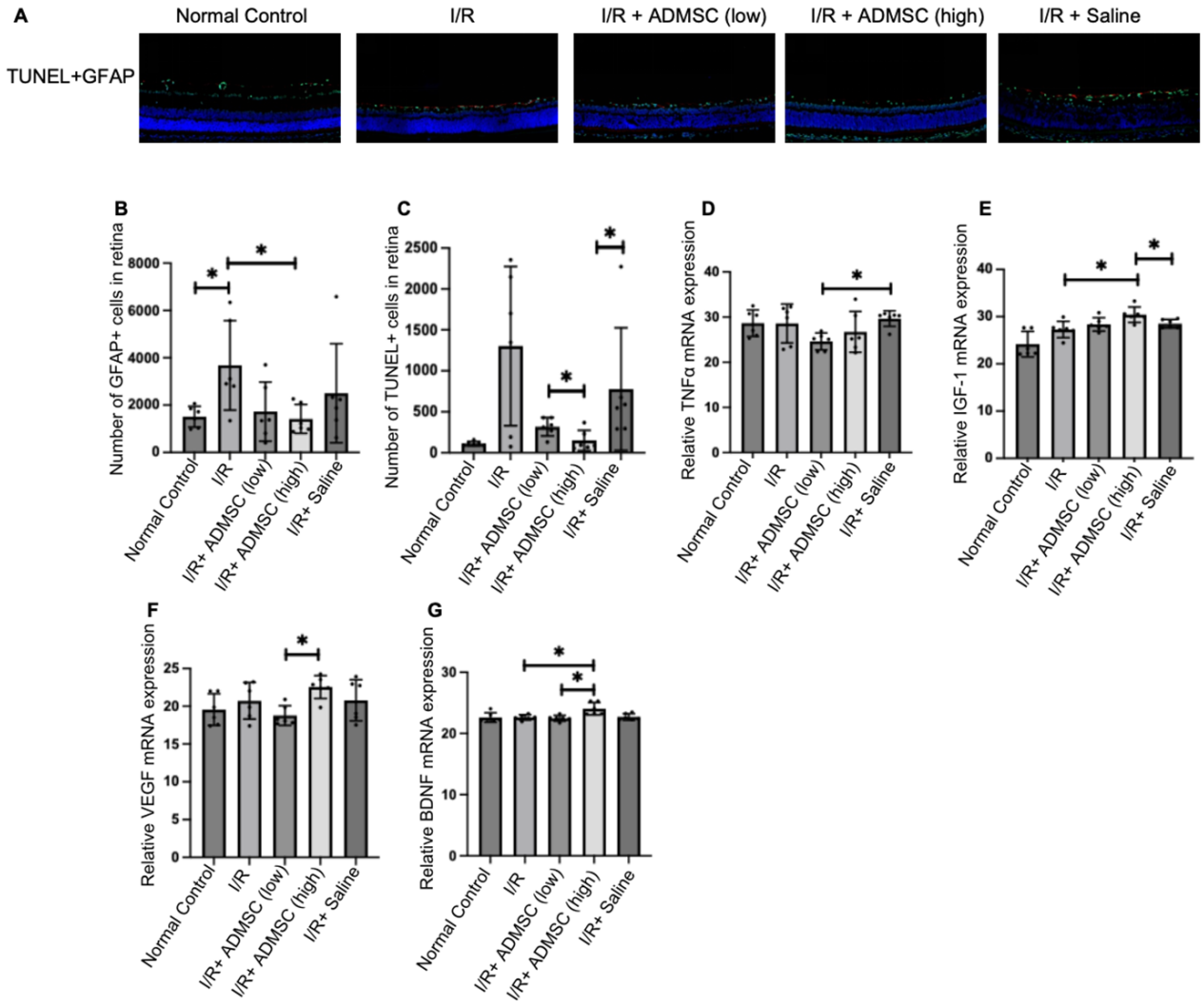

Figure 2. (A) Representative immunofluorescence images of TUNEL and GFAP staining in the retinas of the five groups; GFAP staining is shown in red, while TUNEL-positive cells are shown in green. (B-C) Quantitative analysis of GFAP-positive cells and TUNEL-positive cells in the whole eyeball of each group. (D-F) mRNA expression levels of TNFα, IGF-1, VEGF, and BDNF in the five groups (n = 6, * $p < 0.05$).

nantly located in the nerve fiber layer (NFL) and the ganglion cell layer (GCL) (Figure 2A). Quantification of GFAP-positive cell activation across the entire eye showed mean activated cell counts of 1, 417.17 ± 610.01 and 1,729.17 ± 1,245.00 in the I/R+ADMSC high-dose and low-dose groups, respectively, whereas the mean activated cell count was 2,503.83 ± 2,095.19 in the I/R+Saline group and 3,680.33 ± 1,890.77 in the I/R group (n = 6). The I/R+ADMSC high-dose group exhibited a significantly lower GFAP-positive cell count compared to the I/R group (Figure 2B, $p < 0.05$). Although the numbers of activated cells were also reduced in the I/R+ADMSC groups compared to the I/R+Saline group, the difference did not reach statistical significance ($p > 0.05$).

TUNEL staining is a method widely used to detect and quantify apoptosis by identifying fragmented DNA. TUNEL-positive cells were observed in the retinas of rats in all experimental groups. In the I/R+ADMSC groups, no substantial TUNEL+ cells were noted, whereas partial TUNEL positivity was detected in the ganglion cell layer (GCL) and inner plexiform layer (IPL) of the I/R+Saline group (Figure 2A). Compared with the I/R+ADMSC low-dose group (317.83 ± 112.14, n = 6), the I/R+ADMSC high-dose group (150.17 ± 124.38, n = 6) showed a significantly reduced number of TUNEL-positive cells (Figure 2C, $p < 0.05$).

To evaluate inflammatory responses in the retina, we quantified mRNA expression of TNFα by

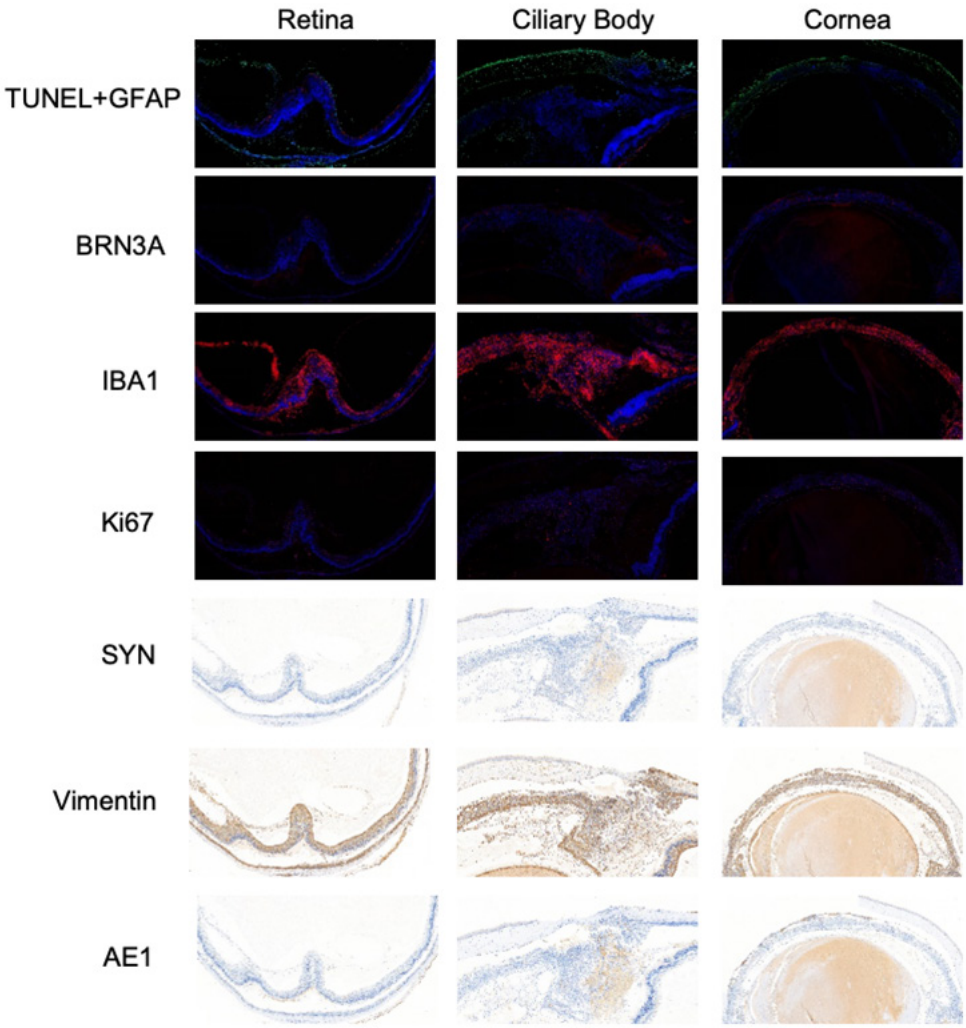

Figure 3. Representative images showing adverse outcomes following vitreous injection of ADMSCs. TUNEL+GFAP, BRN3a, IBA1, and Ki67 were detected using immunofluorescence staining. SYN, Vimentin, and AE1 were detected using immunohistochemical staining.

qPCR. As a pleiotropic cytokine, TNFα is a key molecule in inflammatory signaling [19]. Among the five treatment groups, both ADMSC groups exhibited substantially decreased TNFα expression. However, TNFα expression in the I/R+ADMSC low-dose group was significantly lower than in the I/R+Saline group (Figure 2D, $p < 0.05$). While the I/R+ADMSC low-dose group had lower TNFα expression than the I/R+ADMSC high-dose group, the difference was not statistically significant (Figure 2D, $p > 0.05$).

mRNA expression levels of insulin-like growth factor 1 (IGF-1), vascular endothelial growth factor (VEGF), and brain-derived neurotrophic factor (BDNF) were analyzed in the rat retinas using quantitative polymerase chain reaction (qPCR). Compared with the I/R group, BDNF and IGF-1 expression levels were significantly upregulated in the I/R+ADMSC high-dose group (Figure 2E and 2G, $p < 0.05$). The expression levels of VEGF and BDNF in the I/R+ADMSC high-dose group were significantly higher than in the I/R+ADMSC low-dose group (Figure 2F and 2G, $p < 0.05$). These findings indicate that the I/R+ADMSC high-dose group exhibited stronger neuroprotective effects, and ADMSC administration significantly enhanced the expression of neurotrophic factors in a dose-dependent manner.

Histological examination revealed severe retinal structural disruption in one sample from the I/R+ADMSC high-dose group, including vitreous hemorrhage, anterior chamber hemorrhage, retinal detachment, microglial infiltration, and neovascularization. TUNEL-positive cells were observed in the vitreous cavity and cornea, while GFAP-positive cells were predominantly distributed in the inner plexiform layer (IPL) and above (Figure 3). Under normal conditions, microglia are typically localized

in the ganglion cell layer (GCL), inner plexiform layer (IPL), and outer plexiform layer (OPL). Microglial activation was assessed using BRN3A and IBA1 markers. Immunofluorescence staining revealed that IBA1 expression was detected throughout the retinal layers, predominantly localized above the outer nuclear layer (ONL), with robust expression in the cornea and ciliary body (Figure 3). BRN3A-positive cells were primarily observed in the inner nuclear layer (INL) and the detached retinal interstitium, with partial expression in the cornea (Figure 3).

Intravitreal ADMSC transplantation induced a pronounced inflammatory response, including microglial infiltration, vitreous hemorrhage, retinal detachment, and extensive cellular infiltration, resembling uveitis-like changes. The Ki-67 antigen (Ki67), a nuclear protein expressed during cell proliferation, was detected in the retina, retinal space, vitreous cavity, ciliary body, and cornea (Figure 3), with an activation rate of 13.18% (++). These findings align with significant tissue remodeling and inflammation.

Immunohistochemical analysis of synaptophysin (SYN), vimentin, and cytokeratin AE1 further confirmed alterations in tissue differentiation. AE1, an epithelial differentiation marker, exhibited strong positive staining in the subretinal cavity, detached retina, ciliary body, and cornea (Figure 3). Synaptophysin (SYN), a neuronal marker, displayed localized positivity near the ciliary body, while vimentin, a mesenchymal marker, was strongly expressed throughout the entire tissue (Figure 3). The high expression of vimentin suggests active mesenchymal remodeling, potentially indicative of an inflammation-driven repair process.

Discussion

This study explores the therapeutic effects and potential adverse reactions of intravitreal ADMSC transplantation in a rat model of retinal ischemia-reperfusion (I/R) injury. We observed that the ADMSC treatment group significantly elevated the levels of neurotrophic factors (VEGF, BDNF, IGF-1) and reduced the expression of inflammatory cytokine TNF-α, which is consistent with the known neuroprotective and immunomodulatory roles of stem cells [20, 21]. Notably, the high-dose group exhibited significantly higher levels of BDNF and IGF-1 than the low-dose group, suggesting that high-dose ADMSCs may further enhance retinal repair and neuroprotection by increasing the expression of neurotrophic factors.

In contrast, despite the lower retinal nerve damage scores in the stem cell treatment group, we did not observe significant structural differences between the stem cell and control groups in toluidine blue staining. None of the groups fully recovered to normal retinal architecture. This may be attributed to several factors: first, the study utilized a single time point (4 weeks post-injury), potentially missing the peak period of stem cell efficacy or tissue repair. Second, the administered stem cell dose and frequency may not have been sufficient to fully reverse the severe ischemia-reperfusion injury. Additionally, the variability in the severity of nerve injury within groups may have masked subtle improvements brought about by stem cell therapy.

Nevertheless, ADMSC treatment exhibited clear therapeutic effects in reducing retinal cell apoptosis and improving neurotrophic factor expression. This suggests that stem cell transplantation holds potential for retinal repair, particularly in neuroprotection and regeneration.

At the same time, this study also observed localized structural disorganization, microglial activation, and limited proliferative changes in retinal tissue, resembling uveitis-like reactions. These findings suggest that ADMSC transplantation may induce some degree of inflammation and abnormal proliferation, which requires further investigation to ensure clinical safety. Complications such as retinal detachment, vitreous hemorrhage, and localized proliferation were observed, which is consistent with previous reports [11, 22, 23]. These adverse outcomes may be associated with inflammation and excessive tissue remodeling during the stem cell transplantation process. The observed partial activation of Ki67 and elevated expression of vimentin and AE1 suggest localized cellular proliferation and mesenchymal activity in the retinal and vitreous regions following ADMSC transplantation. These changes may reflect a reparative process initiated by ADMSCs, consistent with their known role in promoting tissue remodeling and neuroprotection [24, 25]. The increased expression of synaptophysin further supports the hypothesis that ADMSCs may enhance neurogenesis or synaptic activity in the retinal ganglion cell layer. However, the high expression of AE1 in non-epithelial tissues and localized Ki67 activation warrant further research to rule out potential pathological proliferative responses. The concurrent expression of vimentin and AE1 in fibroproliferative regions, along with localized Ki67 activation, raises the possibility of abnormal

proliferative processes. Especially in the high-dose group, although neurotrophic factor expression was enhanced, localized proliferative changes, microglial infiltration, and structural damage in retinal tissue suggest that high-dose ADMSCs may lead to more significant inflammatory responses and tissue damage. The increased Ki67 expression and structural disorganization in certain regions highlight the need for further exploration to determine whether these changes are solely inflammatory or involve tumorigenic mechanisms. Therefore, further studies should investigate the dose-dependent effects and long-term safety to determine the optimal therapeutic window for stem cell therapy at different doses [26-29].

Moreover, this study employed intravitreal injection as the method of ADMSC transplantation, which, although currently a common approach for ocular disease therapies, may provoke significant immune responses, including retinal structural disorganization and fibrous tissue proliferation [20, 23]. In contrast, other routes, such as sub-tenon or subretinal injection, may mitigate these adverse effects and improve the integration of transplanted cells with target tissues [4, 30]. Therefore, future studies should systematically compare the safety and efficacy of different injection methods and explore ways to maximize the therapeutic effects of stem cells while minimizing adverse reactions caused by the route of administration.

The limitations of this study include the lack of long-term follow-up and functional assessments, which prevented a full characterization of the proliferative and differentiation-related processes observed. Future studies should employ molecular analysis, long-term monitoring, and additional control groups (e.g., non-I/R, ADMSC-treated eyes) to further elucidate the complete effects mediated by ADMSCs, including the potential risk of pathological proliferation. Additionally, using additional markers for cell proliferation and differentiation will provide a more comprehensive understanding of the observed changes [31-33].

Additionally, the sample size in this study was relatively small, particularly in the control groups. While a larger sample size for the I/R+ADMSC groups, which included two dose subgroups, was necessary for evaluating dose-dependent effects, the smaller sample size in the control groups may have introduced variability in the comparisons across groups. Future studies should consider balancing sample sizes across all groups to improve consistency in inter-group comparisons. Despite this limitation, the consistent trends observed across the analyses support the robustness of the conclusions [30, 34, 35].

In conclusion, while ADMSCs demonstrated significant neuroprotective effects in retinal injury, adverse outcomes such as inflammation and structural disorganization were observed. These findings highlight the importance of rigorously evaluating ADMSC safety and efficacy, particularly under pathological conditions. Modulating immune and inflammatory responses is a promising strategy for minimizing adverse effects and enhancing the therapeutic potential of ADMSC transplantation for retinal diseases [36, 37]. The differential responses between the two tested doses underscore the importance of identifying a therapeutic window that maximizes neuroprotective effects while minimizing adverse outcomes. Translating these results into human clinical practice requires considering species-specific differences in immune response and retinal anatomy. Future studies should focus on optimizing dosage strategies and injection techniques tailored to human conditions to reduce tumorigenic risks and inflammatory responses. Ultimately, further research with multiple time points, larger sample sizes, and long-term safety assessments will be essential to fully elucidate the role of ADMSCs in retinal and optic nerve repair [30, 38, 39].

Abbreviations

adipose mesenchymal stem cells: ADMSCs
brain-derived neurotrophic factor: BDNF
central nervous system: CNS
ischemia/reperfusion: I/R
insulin-like growth factor 1: IGF-1
tumor necrosis factor-alpha: TNF-α
retinal ganglion cells: RGCs
vascular endothelial growth factor: VEGF

ACKNOWLEDGEMENTS

We would like to thank [Beijing Regenerative Biotechnology Research Institute Co., Ltd. (No. H65469-05)] for providing the stem cells used in this study.

Foundations: Supported by Science & Technology, Department of Sichuan Province (No.2021YFS0214).

Conflicts of Interest: The authors declare no competing interests.

References

1. Cui Y, Liu C, Huang L, Chen J, Xu N: **Protective effects of intravitreal administration of mesenchymal stem cell-derived exosomes in an experimental model of optic nerve injury**. *Exp Cell Res* 2021, **407**(1):112792. doi:10.1016/j.yexcr.2021.112792:
2. Almasieh M, Wilson AM, Morquette B, Cueva Vargas JL, Di Polo A: **The molecular basis of retinal ganglion cell death in glaucoma**. *Prog Retin Eye Res* 2012, **31**(2):152-181. doi:10.1016/j.preteyeres.2011.11.002:
3. Johnson TV, DeKorver NW, Levasseur VA, Osborne A, Tassoni A, Lorber B, Heller JP, Villasmil R, Bull ND, Martin KR *et al*: **Identification of retinal ganglion cell neuroprotection conferred by platelet-derived growth factor through analysis of the mesenchymal stem cell secretome**. *Brain* 2014, **137**(Pt 2):503-519. doi:10.1093/brain/awt292: PMC3914467.
4. Huang H, Kolibabka M, Eshwaran R, Chatterjee A, Schlotterer A, Willer H, Bieback K, Hammes HP, Feng Y: **Intravitreal injection of mesenchymal stem cells evokes retinal vascular damage in rats**. *Faseb j* 2019, **33**(12):14668-14679. doi:10.1096/fj.201901500R:
5. Uccelli A, Moretta L, Pistoia V: **Mesenchymal stem cells in health and disease**. *Nat Rev Immunol* 2008, **8**(9):726-736. doi:10.1038/nri2395:
6. Cen J, Zhang Y, Bai Y, Ma S, Zhang C, Jin L, Duan S, Du Y, Guo Y: **Research progress of stem cell therapy for endometrial injury**. *Mater Today Bio* 2022, **16**:100389. doi:10.1016/j.mtbio.2022.100389: PMC9403503.
7. Johnson TV, Bull ND, Martin KR: **Identification of barriers to retinal engraftment of transplanted stem cells**. *Invest Ophthalmol Vis Sci* 2010, **51**(2):960-970. doi:10.1167/iovs.09-3884: PMC2868445.
8. Al-Ghadban S, Bunnell BA: **Adipose Tissue-Derived Stem Cells: Immunomodulatory Effects and Therapeutic Potential**. *Physiology (Bethesda)* 2020, **35**(2):125-133. doi:10.1152/physiol.00021.2019:
9. Pajoohesh-Ganji A, Miller RH: **Targeted Oligodendrocyte Apoptosis in Optic Nerve Leads to Persistent Demyelination**. *Neurochem Res* 2020, **45**(3):580-590. doi:10.1007/s11064-019-02754-z: PMC7058578.
10. Wen YT, Ho YC, Lee YC, Ding DC, Liu PK, Tsai RK: **The Benefits and Hazards of Intravitreal Mesenchymal Stem Cell (MSC) Based-Therapies in the Experimental Ischemic Optic Neuropathy**. *Int J Mol Sci* 2021, **22**(4). doi:10.3390/ijms22042117: PMC7924624.
11. Johnson TV, Bull ND, Martin KR: **Transplantation prospects for the inner retina**. *Eye (Lond)* 2009, **23**(10):1980-1984. doi:10.1038/eye.2008.376:
12. Tassoni A, Gutteridge A, Barber AC, Osborne A, Martin KR: **Molecular Mechanisms Mediating Retinal Reactive Gliosis Following Bone Marrow Mesenchymal Stem Cell Transplantation**. *Stem Cells* 2015, **33**(10):3006-3016. doi:10.1002/stem.2095: PMC4832383.
13. Kahraman NS, Gonen ZB, Sevim DG, Oner A: **First Year Results of Suprachoroidal Adipose Tissue Derived Mesenchymal Stem Cell Implantation in Degenerative Macular Diseases**. *Int J Stem Cells* 2021, **14**(1):47-57. doi:10.15283/ijsc20025: PMC7904524.
14. Özmert E, Arslan U: **Management of retinitis pigmentosa by Wharton's jelly derived mesenchymal stem cells: preliminary clinical results**. *Stem Cell Res Ther* 2020, **11**(1):25. doi:10.1186/s13287-020-1549-6: PMC6958670.
15. Park M, Kim HC, Kim O, Lew H: **Human placenta mesenchymal stem cells promote axon survival following optic nerve compression through activation of NF-κB pathway**. *J Tissue Eng Regen Med* 2018, **12**(3):e1441-e1449. doi:10.1002/term.2561:
16. Cohen I, Sivron T, Lavie V, Blaugrund E, Schwartz M: **Vimentin immunoreactive glial cells in the fish optic nerve: implications for regeneration**. *Glia* 1994, **10**(1):16-29. doi:10.1002/glia.440100104:
17. Trakhtenberg EF, Wang Y, Morkin MI, Fernandez SG, Mlacker GM, Shechter JM, Liu X, Patel KH, Lapins A, Yang S *et al*: **Regulating Set-β's Subcellular Localization Toggles Its Function between Inhibiting and Promoting Axon Growth and Regeneration**. *J Neurosci* 2014, **34**(21):7361-7374. doi:10.1523/jneurosci.3658-13.2014: PMC4028506.
18. Zhao T, Li Y, Tang L, Li Y, Fan F, Jiang B: **Protective effects of human umbilical cord blood stem cell intravitreal transplantation against optic nerve injury in rats**. *Graefes Arch Clin Exp Ophthalmol* 2011, **249**(7):1021-1028. doi:10.1007/s00417-011-1635-7:

19. Chen X, Zhou H, Gong Y, Wei S, Zhang M: **Early spatiotemporal characterization of microglial activation in the retinas of rats with streptozotocin-induced diabetes**. *Graefes Arch Clin Exp Ophthalmol* 2015, **253**(4):519-525. doi:10.1007/s00417-014-2727-y:
20. Adak S, Magdalene D, Deshmukh S, Das D, Jaganathan BG: **A Review on Mesenchymal Stem Cells for Treatment of Retinal Diseases**. *Stem Cell Rev Rep* 2021, **17**(4):1154-1173. doi:10.1007/s12015-020-10090-x: PMC7787584.
21. Ma S, Xie N, Li W, Yuan B, Shi Y, Wang Y: **Immunobiology of mesenchymal stem cells**. *Cell Death Differ* 2014, **21**(2):216-225. doi:10.1038/cdd.2013.158: PMC3890955.
22. Streit WJ, Graeber MB, Kreutzberg GW: **Functional plasticity of microglia: a review**. *Glia* 1988, **1**(5):301-307. doi:10.1002/glia.440010502:
23. Kuriyan AE, Albini TA, Townsend JH, Rodriguez M, Pandya HK, Leonard RE, 2nd, Parrott MB, Rosenfeld PJ, Flynn HW, Jr., Goldberg JL: **Vision Loss after Intravitreal Injection of Autologous "Stem Cells" for AMD**. *N Engl J Med* 2017, **376**(11):1047-1053. doi:10.1056/NEJMoa1609583: PMC5551890.
24. Noorani I, Petty G, Grundy PL, Sharpe G, Willaime-Morawek S, Harris S, Thomas GJ, Nicoll JA, Boche D: **Novel association between microglia and stem cells in human gliomas: A contributor to tumour proliferation?** *J Pathol Clin Res* 2015, **1**(2):67-75. doi:10.1002/cjp2.7: PMC4858136.
25. Chen H, Deng Y, Gan X, Li Y, Huang W, Lu L, Wei L, Su L, Luo J, Zou B *et al*: **NLRP12 collaborates with NLRP3 and NLRC4 to promote pyroptosis inducing ganglion cell death of acute glaucoma**. *Mol Neurodegener* 2020, **15**(1):26. doi:10.1186/s13024-020-00372-w: PMC7161290.
26. Garcia-Valenzuela E, Sharma SC, Piña AL: **Multilayered retinal microglial response to optic nerve transection in rats**. *Mol Vis* 2005, **11**:225-231.
27. Dong N, Chang L, Wang B, Chu L: **Retinal neuronal MCP-1 induced by AGEs stimulates TNF-α expression in rat microglia via p38, ERK, and NF-κB pathways**. *Mol Vis* 2014, **20**:616-628. PMC4016805.
28. Block ML, Zecca L, Hong JS: **Microglia-mediated neurotoxicity: uncovering the molecular mechanisms**. *Nat Rev Neurosci* 2007, **8**(1):57-69. doi:10.1038/nrn2038:
29. Wan P, Su W, Zhang Y, Li Z, Deng C, Li J, Jiang N, Huang S, Long E, Zhuo Y: **LncRNA H19 initiates microglial pyroptosis and neuronal death in retinal ischemia/reperfusion injury**. *Cell Death Differ* 2020, **27**(1):176-191. doi:10.1038/s41418-019-0351-4: PMC7206022.
30. Tuekprakhon A, Sangkitporn S, Trinavarat A, Pawestri AR, Vamvanij V, Ruangchainikom M, Luksanapruksa P, Pongpaksupasin P, Khorchai A, Dambua A *et al*: **Intravitreal autologous mesenchymal stem cell transplantation: a non-randomized phase I clinical trial in patients with retinitis pigmentosa**. *Stem Cell Res Ther* 2021, **12**(1):52. doi:10.1186/s13287-020-02122-7: PMC7796606.
31. Zhao J, Chen M, Xu H: **Experimental autoimmune uveoretinitis (EAU)-related tissue damage and angiogenesis is reduced in CCL2$^{-/-}$ CX$_3$CR1gfp/gfp mice**. *Invest Ophthalmol Vis Sci* 2014, **55**(11):7572-7582. doi:10.1167/iovs.14-15495:
32. Mendiola AS, Garza R, Cardona SM, Mythen SA, Lira SA, Akassoglou K, Cardona AE: **Fractalkine Signaling Attenuates Perivascular Clustering of Microglia and Fibrinogen Leakage during Systemic Inflammation in Mouse Models of Diabetic Retinopathy**. *Front Cell Neurosci* 2016, **10**:303. doi:10.3389/fncel.2016.00303: PMC5222852.
33. Kinuthia UM, Wolf A, Langmann T: **Microglia and Inflammatory Responses in Diabetic Retinopathy**. *Front Immunol* 2020, **11**:564077. doi:10.3389/fimmu.2020.564077: PMC7681237.
34. Tan J, Zhang X, Li D, Liu G, Wang Y, Zhang D, Wang X, Tian W, Dong X, Zhou L *et al*: **scAAV2-Mediated C3 Transferase Gene Therapy in a Rat Model with Retinal Ischemia/Reperfusion Injuries**. *Mol Ther Methods Clin Dev* 2020, **17**:894-903. doi:10.1016/j.omtm.2020.04.014: PMC7200613.
35. Wang Z: **Assessing Tumorigenicity in Stem Cell-Derived Therapeutic Products: A Critical Step in Safeguarding Regenerative Medicine**. *Bioengineering (Basel)* 2023, **10**(7). doi:10.3390/bioengineering10070857: PMC10376867.
36. Altmann C, Schmidt MHH: **The Role of Microglia in Diabetic Retinopathy: Inflammation, Microvasculature Defects and Neurodegeneration**. *Int J Mol Sci* 2018, **19**(1). doi:10.3390/ijms19010110: PMC5796059.

37. Li L, Heiduschka P, Alex AF, Niekämper D, Eter N: **Behaviour of CD11b-Positive Cells in an Animal Model of Laser-Induced Choroidal Neovascularisation**. *Ophthalmologica* 2017, **237**(1):29-41. doi:10.1159/000453550:
38. Wagner N, Reinehr S, Palmhof M, Schuschel D, Tsai T, Sommer E, Frank V, Stute G, Dick HB, Joachim SC: **Microglia Activation in Retinal Ischemia Triggers Cytokine and Toll-Like Receptor Response**. *J Mol Neurosci* 2021, **71**(3):527-544. doi:10.1007/s12031-020-01674-w: PMC8575759.
39. Yang Z, Liu Y, Chen X, Huang S, Li Y, Ye G, Cao X, Su W, Zhuo Y: **Empagliflozin targets Mfn1 and Opa1 to attenuate microglia-mediated neuroinflammation in retinal ischemia and reperfusion injury**. *J Neuroinflammation* 2023, **20**(1):296. doi:10.1186/s12974-023-02982-9: PMC10714482.